ACS APPLIED MATERIALS & INTERFACES

Research Article

www.acsami.org

Biocompatible Flavone-Based Fluorogenic Probes for Quick Wash-Free Mitochondrial Imaging in Living Cells

Bin Liu,[†] Mickey Shah,[‡] Ge Zhang,[‡] Qin Liu,[§] and Yi Pang*[,†]

[†]Department of Chemistry and Maurice Morton Institute of Polymer Science, [‡]Department of Biomedical Engineering, and [§]Department of Biology, The University of Akron, Akron, Ohio 44325, United States

Supporting Information

ABSTRACT: Mitochondria, vital organelles existing in almost all eukaryotic cells, play a crucial role in energy metabolism and apoptosis of aerobic organisms. In this work, we report two new flavone-based fluorescent probes, **MC-Mito1** and **MC-Mito2**, for monitoring mitochondria in living cells. These two probes exhibit remarkably low toxicity, good cell permeability, and high specificity; these probes complement the existing library of mitochondrial imaging agents. The new dyes give nearly no background fluorescence, and their application does not require tedious postwashing after cell staining. The appreciable tolerance of **MC-Mito2** encourages a broader range of biological applications for understanding the cell degeneration and apoptosis mechanism.

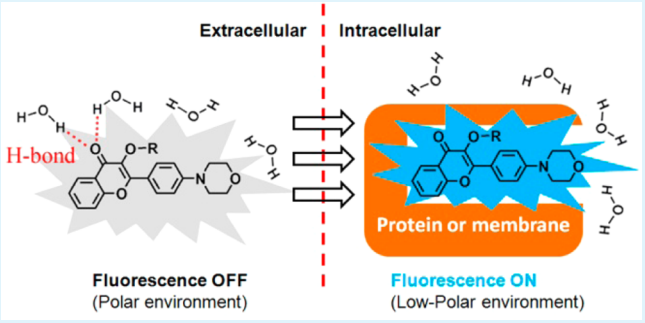

KEYWORDS: *imaging agents, fluorescence, mitochondria, flavone, biocompatibility, wash-free*

INTRODUCTION

Monitoring the biomolecular and biochemical process in organisms is a fundamental issue in biosensing, with applications from fundamental biological research to clinical diagnostics.[1−3] Mitochondria, membrane-bound organelles found in most eukaryotic cells,[4] play important roles in numerous vital cellular processes, such as energy supply, reactive oxygen species generation, signaling, cellular differentiation, and cell death.[5] The mitochondrial network displays remarkable plasticity during the development of certain tissues. The morphology of mitochondria is affected by cell type, cell cycle stage, and intracellular metabolic state, which in turn contributes to cell functioning.[6] Recent reports show that the mitochondria are also crucially involved in various pathologies, from Alzheimer's disease to cancer.[7,8] Thus, development of a convenient and efficient mitochondrial imaging method is of great fundamental importance for understanding the cell biochemistry process and early diagnosis of disease.

Fluorescence techniques are particularly well suited for biological application, because they are noninvasive and highly sensitive. So far, a few fluorescent dyes have been developed for mitochondrial imaging, such as rhodamines,[9,10] rosamines,[11,12] carbocyanines,[13] and BODIPY dyes,[14−17] with some showing two-photon emission (TPE) properties.[18−22] However, most mitochondrial probes, such as BODIPY dyes, give strong fluorescence signals in a buffer solution. During the application, the unbound probes must be washed off to eliminate the strong residual signal from the free dyes to improve the signal-to-noise (S/N) ratio. The time-consuming washing process will inevitably delay the acquisition of microscopic data.[23] In addition, the required postapplication washing procedure could alter the cell environment and hamper the probe's ability to monitor mitochondrial changes in real time because the number and subcellular locations of mitochondria dramatically change with the cell's metabolic demands.[24,25] Moreover, because mitochondria are directly associated with cytoactivity, the dying cells could be removed during the washing process, adversely affecting the monitoring of the whole cell apoptosis cycle.[26] To overcome this deficiency, aggregation-induced emission (AIE) dyes[27,28] have been used to minimize the fluorescence signals of free dyes. The use of AIE dyes, however, requires the significant accumulation of dye molecules on the cells to cause aggregation. Developing a novel strategy that permits specific mitochondrial labeling without the postapplication washing, thereby allowing continuous observation of the entire biochemistry process without interruption, remains a challenge. Although an AIE dye has been used to track the mitochondria without a washing process,[28] it is desirable to identify a new mechanism that does not require the accumulation of dye molecules on the cells, which usually takes a longer time (e.g., 20 min) and a high concentration to stain the target.

Environmentally sensitive fluorophores represent a class of interesting dyes whose emission properties are highly sensitive to their immediate environment.[29−31] These dyes can exhibit scarce fluorescence in polar solvents but become highly

Received: September 29, 2014
Accepted: November 7, 2014
Published: November 7, 2014

fluorescent in weakly polar solvents,[32] so they could be the ideal candidates for a no-wash assay. Among the environmentally sensitive fluorophores, flavones have exhibited classical positive solvatochromism features.[33,34] Because the highly polar water molecule is a strong H-bond donor, the fluorescence of flavones can be severely quenched by the intermolecular electron or proton transfer between dyes and water (Figure 1).[35] The fluorescence of flavones could be efficiently switched

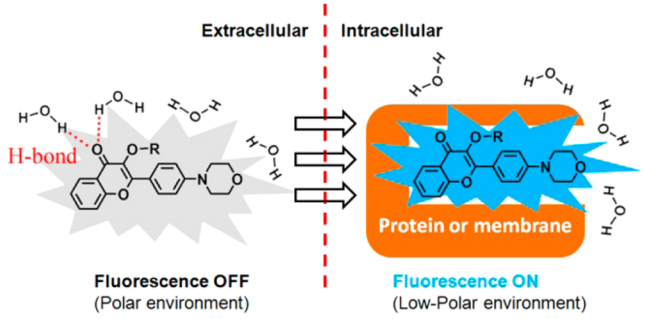

Figure 1. Wash-free fluorescence imaging method based on flavone dyes.

on when they are incorporateded by proteins or lipid membranes into the nonpolar microenvironment in cells. With the reasoning described above, we assume that flavone probes could offer attractive features in mitochondrial imaging. In the new sensor design of **MC-Mito1** and **MC-Mito2**, the environmentally sensitive flavone dyes are conjugated with a mitochondrion-targeting group triphenylphosphonium. Interestingly, the probes show a large turn-on upon binding to mitochondria. Because the probes are nearly nonfluorescent in the aqueous environment, their application no longer requires tedious postwashing. In addition, as a broad class of natural products,[36,37] the flavone-based dyes show very low toxicity toward living stem cells and could specifically label mitochondria with a short incubation time.

EXPERIMENTAL SECTION

Synthesis. *3-Hydroxy-2-(4-morpholinophenyl)-4H-chromen-4-one (**MC**).* 2-Hydroxyacetophenone (2.72 g, 20 mmol) was added to a solution of the 4-morpholinobenzaldehyde (3.82 g, 20 mmol) in ethanol (40 mL), and then 20 mL of an aqueous NaOH (8 g) solution was added slowly. The mixture was stirred at room temperature for 24 h. A H_2O_2 solution (8 mL of 30%) was slowly added to the reaction solution, which was placed in an ice−water bath. After being stirred at room temperature for 10 h, the mixture was poured into an ice−water bath, and the precipitate was collected via filtration and washed with ethanol. The product was purified by recrystallization from ethanol: yield 41%; ^{1}H NMR (DMSO-d_6, 300 MHz) δ 8.176 (d, J = 9.0 Hz, 2H), 8.087 (d, J = 7.5 Hz, 1H), 7.775 (m, 2H), 7.447 (m, 1H), 7.091 (d, J = 9.3 Hz, 2H), 3.763 (t, 4H), 3.265 (t, 4H); ^{13}C NMR (DMSO-d_6, 75 MHz) δ 173.063, 154. 741, 151.999, 146.507, 138.894, 133.555, 129.264, 125.183, 124.773, 121.855, 121.617, 118.636, 114.369, 66.370, 47.707.

*{3-[2-(4-Morpholinophenyl)-4-oxo-4H-chromen-3-yloxy]propyl}-triphenylphosphonium Bromide (**MC-Mito1**).* 3-Hydroxy-2-(4-morpholinophenyl)-4*H*-chromen-4-one (**MC**) (0.646 g, 2 mmol), $CsCO_3$ (1.63 g, 5 mmol), (3-bromopropyl)triphenylphosphonium bromide (4.61 g, 10 mmol), and tetrabutylammonium bromide (1.61 g, 5 mmol) were dissolved in 10 mL of dimethylformamide (DMF). The mixture was stirred at room temperature for 72 h, and the resulting product was poured into water. The product mixture was extracted with 20 mL of DCM and dried with Na_2SO_4. After concentration under reduced pressure, the residue was purified by column chromatography (10:1 CH_2Cl_2/MeOH) to afford a white solid: yield 55%; ^{1}H NMR ($CDCl_3$, 300 MHz) δ 8.150 (d, J = 8.1 Hz, 1H), 8.000 (d, J = 9.0 Hz, 2H), 7.851−7.673 (m, 16H), 7.515 (d, J = 8.1 Hz, 1H), 7.369 (t, 1H), 6.999 (d, J = 9.0 Hz, 2H), 4.236 (t, 2H), 4.110 (t, 2H), 3.871 (t, 4H), 3.271 (t, 4H), 2.214 (m, 2H); ^{13}C NMR ($CDCl_3$, 75 MHz) δ 174.788, 156.724, 155.107, 152.626, 139.189, 135.055, 135.015, 134.950, 134.911, 133.881, 133.748, 133.248, 130.499, 130.398, 130.332, 129.951, 125.449, 124.524, 124.007, 120.410, 118.887, 117.954, 117.745, 114.219, 71.459, 66.624, 47.687, 24.263, 19.911; ESI-MS for $C_{40}H_{37}NO_4P^+$ [M^+] calcd 626.2455, found 626.2457.

*3-(6-Bromohexyloxy)-2-(4-morpholinophenyl)-4H-chromen-4-one (**MC-Br**).* 3-Hydroxy-2-(4-morpholinophenyl)-4*H*-chromen-4-one (**MC**) (1.615 g, 5 mmol), $CsCO_3$ (3.26 g, 10 mmol), tetrabutylammonium bromide (3.22 g, 10 mmol), and 1,6-dibromohexane (6 g, 25 mmol) were added to 40 mL of DMF. The mixture was stirred at room temperature for 72 h and then poured into 200 mL of water. The mixture was extracted with 50 mL of DCM and then washed with brine and water. After concentration under reduced pressure, the residue was purified by column chromatography (1:1 CH_2Cl_2/EtOAc): yield 69%; ^{1}H NMR ($CDCl_3$, 300 MHz) δ 8.262 (dd, J = 8.1 Hz, J = 1.5 Hz, 1H), 8.111 (d, J = 9.3 Hz, 2H), 7.675 (m, 1H), 7.522 (d, J = 8.1 Hz, 1H), 7.401 (m, 1H), 6.997 (d, J = 9.3 Hz, 2H), 4.078 (t, 2H), 3.908 (t, 4H), 3.394 (t, 2H), 3.339 (t, 4H), 1.860−1.725 (m, 4H), 1.475−1.410 (m, 4H); ^{13}C NMR ($CDCl_3$, 75 MHz) δ 174.871, 156.053, 155.118, 152.411, 139.731, 133.006, 130.008, 125.712, 124.400, 123.005, 121.368, 117.774, 113.892, 72.190, 66.643, 47.863, 33.764, 32.787, 29.906, 27.923, 25.176.

*{6-[2-(4-Morpholinophenyl)-4-oxo-4H-chromen-3-yloxy]hexyl}-triphenylphosphonium Bromide (**MC-Mito2**).* 3-(6-Bromohexyloxy)-2-(4-morpholinophenyl)-4*H*-chromen-4-one (**MC-Br**) (0.97 g, 2 mmol), KI (0.33 g, 2 mmol), and triphenylphosphine (2.62 g, 10 mmol) were dissolved in 15 mL of toluene. The mixture was heated to reflux for 4 h and then cooled to room temperature. The mixture was poured into 100 mL of ether to precipitate. The crude product was dissolved in a mixture of 15 mL of DMF and 5 mL of aqueous NaBr (3 g). The mixture was stirred for 3 h at 50 °C, extracted with 50 mL of DCM, and washed with 100 mL of water. The solution was concentrated to 5 mL and poured into 50 mL of ether. The precipitate could be used directly without further purification: yield 63%; ^{1}H NMR ($CDCl_3$, 300 MHz) δ 8.167 (dd, J = 8.1 Hz, J = 1.5 Hz, 1H), 8.087 (d, J = 9.0 Hz, 2H), 7.87−7.609 (m, 16H), 7.519 (d, J = 8.4 Hz, 1H), 7.370 (t, 1H), 7.011 (d, J = 9.3 Hz, 2H), 3.943 (t, 2H), 3.884 (t, 4H), 3.761 (m, 2H), 3.341 (t, 4H), 1.735−1.526 (m, 4H); ^{13}C NMR ($CDCl_3$, 75 MHz) δ 174.844, 156.289, 155.091, 152.516, 139.571, 135.050, 135.012, 133.765, 133.633, 133.046, 130.585, 130.503, 130.419, 129.831, 125.453, 124.375, 124.169, 120.851, 118.810, 117.883, 117.672, 114.027, 71.963, 66.651, 47.773, 30.104, 29.896, 29.579, 25.364, 23.332, 22.471; ESI-MS for $C_{43}H_{43}NO_4P^+$ [M^+] calcd 668.2924, found 668.2913.

Fluorescence Quantum Yield. The fluorescence quantum yields were obtained using rhodamine 6G (sigma) as the standard (Φ_{fl} = 0.95, in ethanol).[38] The fluorescence quantum yields can be calculated by using the following equation:

$$\Phi_s = \Phi_r(A_r n_s^2 F_s)/(A_s n_r^2 F_r) \quad (1)$$

where the subscripts s and r refer to the sample and the standard, respectively, Φ is the quantum yield, F is the integrated emission intensity, A is the absorbance, and n is the refractive index.

Zebrafish Breeding and Imaging. All animal-related procedures were approved by the Care and Use of Animals in Research Committee at The University of Akron. Zebrafish (*Danio rerio*) were maintained as described in the *Zebrafish Book* by Westerfield (2007), University of Oregon. Zebrafish were kept at 28.5 °C and kept under optimal breeding conditions. For mating, male and female zebrafish were maintained in one tank at 28.5 °C on a 12 h light/12 h dark cycle and then the spawning of eggs was triggered by giving light stimulation in the morning. Almost all the eggs were fertilized immediately. The zebrafish were maintained in E3 embryo medium [15 mM NaCl, 0.5 mM KCl, 1 mM $MgSO_4$, 1 mM $CaCl_2$, 0.15 mM

KH_2PO_4, 0.05 mM Na_2HPO_4, 0.7 mM $NaHCO_3$, and 10^{-5}% methylene blue (pH 7.5)]. The 4 h postfertilization (hpf) zebrafish embryos were incubated with E3 medium containing 5 μmol/L **MC-Mito1** and **MC-Mito2** for 15 min. The fluorescence images of embryos were directly taken without washing.

Cell Culture and Imaging. Human mesenchymal stem cells (hMSCs) (Lonza, Walkersville, MD) were cultured in serum-containing MSCBM medium (Lonza) supplemented with MSCGM SingleQuots (Lonza) according to the manufacturer's specifications. hMSCs (passage 5) were seeded at a density of 1×10^4 cells/cm^2. For costaining experiments, the hMSCs were seeded on a 12-well plate, cultured in MSCBM medium (Lonza) supplemented with MSCGM SingleQuots (Lonza), and incubated with 5 μM **MC** and 25 nM Mitotracker red CMXRos (**MT**), 5 μM **MC-Br** and 25 nM **MT**, 5 μM **MC-Mito1** and 25 nM **MT**, and 5 μM **MC-Mito2** and 25 nM **MT** for 25 min at 37 °C. Each well contained 1 mL of medium and 0.05 mL of DMSO (dissolving probe). The cell imaging was obtained on a Zeiss inverted fluorescence microscope with X-Cite Series 120Q. The blue channel filter was as follows: excitation at 365 nm, beam splitter FT at 395 nm, and emission at 445/50 nm. The green channel filter was as follows: excitation at 450–490 nm, beam splitter FT at 510 nm, and emission at 515–565 nm. The red channel filter was as follows: excitation at 587/25 nm, beam splitter FT at 605 nm, and emission at 647/70 nm.

Cytotoxicity Determined by the MTT Method. The hMSCs were seeded in 12-well plates at a density of 5.0×10^4 cells/cm^2. After a 24 h incubation, the cells were exposed to a series of doses of probe **MC-Mito1** or **MC-Mito2** and **MT** at 37 °C. The concentration of MT (0, 2, 5, or 10 μM) was similar to that reported in the literature.[28] After 24 h, the MTT solution (sigma) was added and kept for 3 h in the incubator. The MTT solubilization solution was then added to each well, and the plate was gently shaken for 10 min at room temperature. The absorbance of MTT in the sample well was determined by subtracting the absorbance of the sample well from that of the corresponding control well. Cell viability was expressed as the ratio of the absorbance of MTT in the sample wells to that of the cells incubated with culture medium only.[39]

Effects of Carbonyl Cyanide *m*-Chlorophenylhydrazone (CCCP) on Uptake of Dyes. The hMCSc were treated with 10 μM CCCP for 30 min and then washed with fresh medium. After that, the cells were incubated with 5 μM **MC-Mito1** and 25 nM **MT** or with 5 μM **MC-Mito2** and 25 nM **MT** for 25 min at 37 °C. After being stained, the cells were imaged with a microscope without the PBS solution washing procedure.

RESULTS AND DISCUSSION

MC-Mito1 was synthesized by reaction of (3-bromopropyl)-triphenylphosphonium with 3-hydroxy-2-(4-morpholinophenyl)-4*H*-chromen-4-one (**MC**) (Figure 2), which was obtained in two steps by a Claisen–Schmidt condensation and Algar–Flynn–Oyamada reaction.[40−42] **MC-Mito2** was prepared in two steps from **MC** by conjugation with a longer linker unit, followed by reaction with triphenylphosphine. Both **MC-Mito1** and **MC-Mito2** consist of the flavone fluorophore, alkyl linker, and triphenylphosphonium as the mitochondrion-targeting group. The length of the alkyl linker is known to be crucial for achieving a balanced labeling efficiency and target selectivity for bioimaging.[43] The full synthesis and characterization details of the compounds are given in the Experimental Section and Figures S1–S8 of the Supporting Information.

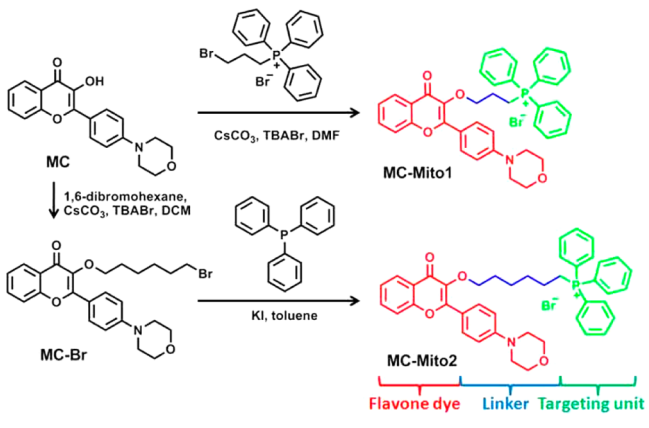

Figure 2. Design and synthesis of **MC-Mito1** and **MC-Mito2**.

In a DMSO solution, **MC-Mito1** and **MC-Mito2** exhibited similar photophysical properties (Figure 3), showing absorption

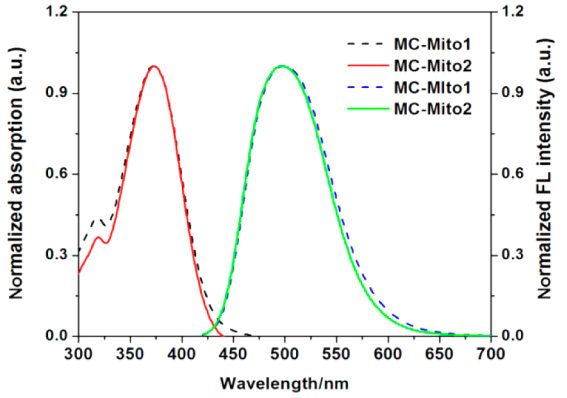

Figure 3. Normalized UV spectra and FL spectra of **MC-Mito1** (dashed lines) and **MC-Mito2** (solid lines) in a DMSO solution.

maxima at 373 nm and emission maxima at 500 nm. The emission spectra of dyes were well separated from the absorption, revealing a large Stokes shift (~127 nm) that is highly desirable for fluorescence imaging. The environmentally sensitive properties of **MC-Mito1** and **MC-Mito2** were examined in different solvents (Figure S9 of the Supporting Information). The results indicate that **MC-Mito1** and **MC-Mito2** showed classical positive solvatochromism features of flavone dyes,[44] with a correlation between the emission maximum and relative solvent polarity. The emission spectra shifted dramatically to longer wavelengths (from 450 to 540 nm) as the solvent polarity was increased. The probe's ability to shift the fluorescence from a polar to nonpolar environment could also facilitate the wash-free application, as the cell-bound dyes gave emission at wavelengths distinct from those of the free dye in an aqueous solution.

MC-Mito1 and **MC-Mito2** were nearly nonfluorescent in water (QY < 1%), because of specific H-bonding interactions of water solvents with H-bond acceptor carbonyl groups in a flavone skeleton.[44] However, upon addition of bovine serum albumin (BSA) to the probe water solution, the fluorescence intensity increased sharply (Figure 4). After addition of 2 equiv of BSA, the fluorescence intensity of **MC-Mito1** at 495 nm was enhanced by ~17-fold, which was accompanied by a large blue-shift [from 540 to 495 nm (Figure 4a,b)]. The fluorescence intensity of **MC-Mito2** at 490 nm was dramatically enhanced by ~55-fold upon addition of 2 equiv of BSA, accompanied by 50 nm blue-shift, as well. By using rhodamine 6G in ethanol (QY = 95%)[38] as a reference, the fluorescence quantum yields (QYs) of **MC-Mito1** and **MC-Mito2** were determined to be 28% and 33%, repectively. The photophysical properties of **MC-Mito1** and **MC-Mito2** thus point to the potential of achieving wash-free imaging methods, which normally require

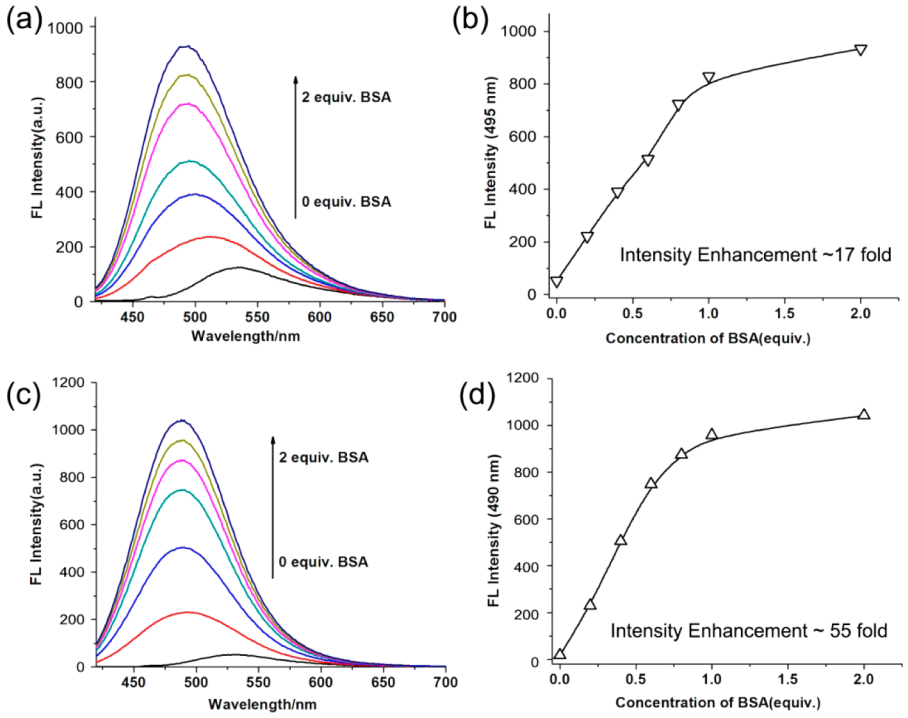

Figure 4. Fluorescence response of probes **MC-Mito1** (a) and **MC-Mito2** (c) upon addition of different concentrations of BSA in 1 mM HEPES buffer (1% DMSO). Fluorescence intensity changes of **MC-Mito1** (b) and **MC-Mito2** (d) in the presence of increasing concentrations of BSA in 1 mM HEPES buffer (1% DMSO). [**MC-Mito1**] = [**MC-Mito2**] = 2 μM. [BSA] = 0–4 μM. λ_{ex} = 400 nm.

the probe to possess the following properties: (1) the fluorophore should be nonfluorescent (or weakly fluorescent) in water medium, and (2) the fluorescence can be turned on when the fluorophore crosses the cell membrane into a weakly polar intracellular environment, which is essential for a high signal-to-noise ratio.[23] To simply verify the imaging properties of these two dyes, zebrafish embryos 4 h postfertilization were stained with 5 μM **MC-Mito1** and **MC-Mito2** for 15 min and then directly used for imaging without a washing process (Figure S10 of the Supporting Information). The images clearly show the fluorescence outline around the embryos and a very weak background signal. The high signal-to-noise ratio (>10) allows simple wash-free *in vivo* fluorescence imaging.

Before the application for cell imaging, the cytotoxicities of **MC-Mito1** and **MC-Mito2** were evaluated by the widely used MTT assay to evaluate the tolerance of sensors to their working concentrations. The samples were incubated with 0, 2, 5, or 10 μM **MC-Mito1**, **MC-Mito2**, and Mitotracker red CMXRos (**MT**) for 24 h (Figure 5). The results show that the cell viabilities of **MC-Mito1** and **MC-Mito2** were close to 100%. In contrast, only less than 10% of the cells were viable after incubation with 5 μM commercial mitochondrial dye **MT** for 24 h. These results indicate that the wider working concentrations of **MC-Mito1** and **MC-Mito2** were much easier to manipulate in bioimaging than those of commercial **MT**, which tends to lose specificity and even cause cell apoptosis at higher concentrations.[27]

To assess their cell staining efficiencies, the hMSCs cells were incubated with **MT**, **MC-Mito1**, and **MC-Mito2**, (Figure S11 of the Supporting Information). Cell staining was continuously recorded for 3, 10, and 25 min without a washing process. We found **MC-Mito1** and **MC-Mito2** could quickly stain the living cells in 10 min. In contrast, the **MT** required a longer time to efficiently stain cells. The fluorescence signals of **MC-Mito1**

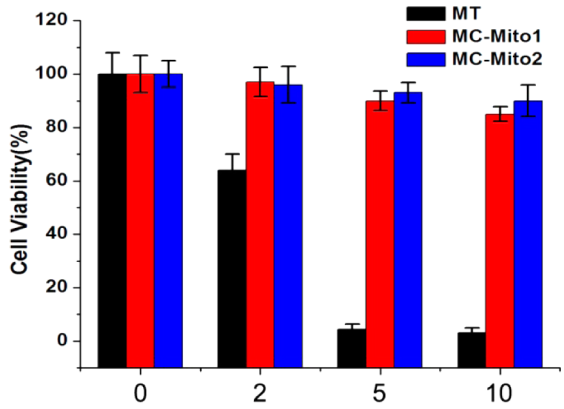

Figure 5. Cytotoxicity experiments with **MC-Mito1**, **MC-Mito2**, and **MT** at various concentrations in hMSCs (0, 2, 5, and 10 μM) for 24 h.

and **MC-Mito2** from the "blue channel" on a fluorescence microscope (420–470 nm) were confined in cells with a negligible background signal from the culture medium, supporting the hypothesis that the flavone dyes gave greater emission in a weakly polar environment. In general, the S/N ratios in fluorescent images were >3, which could be considered acceptable for the discrimination of mitochondria. Therefore, this wash-free method could be a useful probe for monitoring of mitochondrial changes in real time.

To determine the subcellular distribution of the probes in living cells, **MT** was co-incubated with **MC-Mito1** and **MC-Mito2**. Figure 6 shows that the reticulum-like mitochondria were widespread across the entire cytoplasm. The subcellular regions stained with **MC-Mito1** (blue and green channel) matched those stained with **MT** (red channel) very well. Similarly, the **MC-Mito2** staining pattern also matched well that of **MT** (Figure 6g–l). Without the targeting group, **MC**

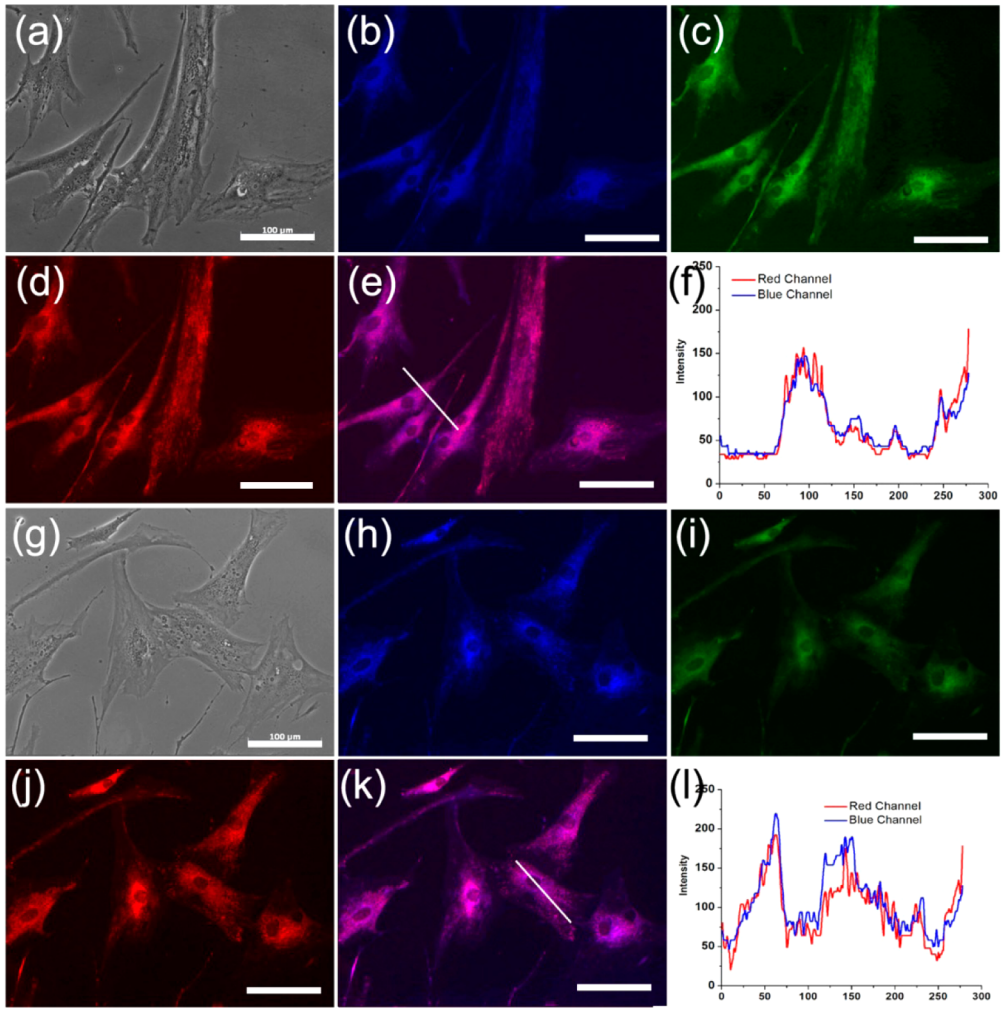

Figure 6. Fluorescence images of hMSCs costained with 25 nM **MT** and 5 μM **MC-Mito1** for 25 min (a–f) and 25 nM **MT** and 5 μM **MC-Mito2** for 25 min (g–l). Bright field (a and g), blue channel (b and h), green channel (c and i), red channel (d and j), overlay images of the blue channel and red channel (e and k), and profiles of locations in the overlay images (f and l). The scale bar is 100 μm.

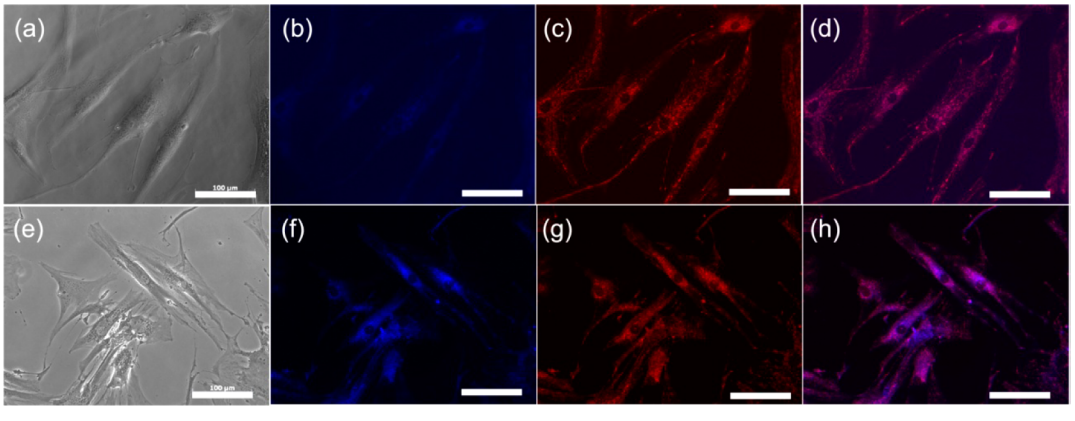

Figure 7. Fluorescence images of hMSCs that were pretreated with 10 μM CCCP for 30 min and then costained with 25 nM **MT** and 5 μM **MC-Mito1** for 25 min (a–d) or 25 nM **MT** and 5 μM **MC-Mito2** for 25 min (f–h). Bright field (a and e), blue channel (b and f), red channel (c and g), and overlay images of the blue channel and red channel (d and h). The scale bar is 100 μm.

and **MC-Br** showed almost no colocalization with **MT** (see Figures S12 and S13 of the Supporting Information), confirming that the mitochondrial targetability of these two probes strongly depends on the triphenylphosphonium group, despite the fact that the decrease in membrane potential will severely affect the direction and accumulation of cationic mitochondrial probes.

Mitochondria can continuously oxidize substrates and maintain a proton gradient across the lipid bilayer with a very large membrane potential (−180 mV).[45] The membrane potential as the major driving force allows the entrance and

accumulation of the cationic species into mitochondria rather than cell plasma.[46] CCCP is an uncoupler that causes rapid acidification of mitochondria and dysfunction of ATP synthase, resulting in a decrease in mitochondrial membrane potential.[47] To confirm the tolerances of **MC-Mito1** and **MC-Mito2**, CCCP was used to treat the cells prior to the staining procedure. Figure 7 shows the fluorescent images of hMSCs after they had been pretreated with 10 μM CCCP for 30 min and stained with probes. It was found that the reticulum-like mitochondria are mostly transformed to small and dispersed fragments, because of the CCCP-induced collapse of the mitochondrial membrane potential associated with the remodeling of mitochondrial cristae and the subsequent occurrence of morphological changes in mitochondria.[48]

After the treatment of CCCP, the uptake of **MT** was decreased by more than half and the specificity became worse (Figure 7c,g). **MC-Mito1** showed an imaging signal much weaker than that in normal cells and almost no more specificity for mitochondria (Figure 7b). It was expected because a CCCP-induced decrease in membrane potential will severely affect the direction and accumulation of cationic mitochondrial probes. The most commercial mitochondrial probes suffer from a similar limitation.[18] However, under the same condition, the specificity and sensitivity of **MC-Mito2** to mitochondria are perfectly retained in CCCP-treated cells (Figure 7f). Compared with that of **MC-Mito1**, the hydrophobic linker between the flavone dye and the cation of **MC-Mito2** is longer. Because mitochondrial membranes are composed of phospholipid bilayers and proteins,[49] the stronger lipophilicity has been thought to play an important role in retaining the specificity of **MC-Mito2** in CCCP-treated cells.[27]

CONCLUSION

In summary, we present two novel flavone-based probes, **MC-Mito1** and **MC-Mito2**, for specific mitochondrial imaging. The probes can be used conviniently to stain living cells without a washing process. Both **MC-Mito1** and **MC-Mito2** possessed significant advantages, such as low toxicity, good cell permeability, high specificity for mitochondria, and real-time continuous monitoring of mitochondrial morphology. Proper chemical modification of **MC-Mito2** made it appreciably tolerant to microenvironmental changes in mitochondria, suggesting it could be a pratical probe for mitochodrial imaging in live cells.

ASSOCIATED CONTENT

Supporting Information

Additional information about reagents and instrumentation and Figures S1−S13. This material is available free of charge via the Internet at http://pubs.acs.org.

AUTHOR INFORMATION

Corresponding Author

*E-mail: yp5@uakron.edu.

Notes

The authors declare no competing financial interest.

ACKNOWLEDGMENTS

This work was supported by National Institutes of Health Grant 1R15EB014546. We also thank the Coleman Endowment of The University of Akron for partial support.

REFERENCES

(1) Yuste, R. Fluorescence microscopy today. *Nat. Methods* **2005**, *2*, 902−904.
(2) Borisov, S. M.; Wolfbeis, O. S. Optical biosensors. *Chem. Rev.* **2008**, *108*, 423−461.
(3) Yang, Y.; Zhao, Q.; Feng, W.; Li, F. Luminescent chemodosimeters for bioimaging. *Chem. Rev.* **2013**, *113*, 192−270.
(4) Henze, K.; Martin, W. Evolutionary biology: Essence of mitochondria. *Nature* **2003**, *426*, 127−128.
(5) McBride, H. M.; Neuspiel, M.; Wasiak, S. Mitochondria: More than just a powerhouse. *Curr. Biol.* **2006**, *16*, R551−R560.
(6) Karbowski, M.; Youle, R. J. Dynamics of mitochondrial morphology in healthy cells and during apoptosis. *Cell Death Differ.* **2003**, *10*, 870−880.
(7) Ow, Y. L. P.; Green, D. R.; Hao, Z.; Mak, T. W. Cytochrome c: Functions beyond respiration. *Nat. Rev. Mol. Cell Biol.* **2008**, *9*, 532−542.
(8) Landes, T.; Martinou, J. C. Mitochondrial outer membrane permeabilization during apoptosis: The role of mitochondrial fission. *Biochim. Biophys. Acta* **2011**, *1813*, 540−545.
(9) Dickinson, B. C.; Lin, V. S.; Chang, C. J. Preparation and use of MitoPY1 for imaging hydrogen peroxide in mitochondria of live cells. *Nat. Protoc.* **2013**, *8*, 1249−1259.
(10) Johnson, L. V.; Walsh, M. L.; Chen, L. B. Localization of Mitochondria in Living Cells with Rhodamine-123. *Proc. Natl. Acad. Sci. U.S.A.* **1980**, *77*, 990−994.
(11) Johnson, L. V.; Walsh, M. L.; Bockus, B. J.; Chen, L. B. Monitoring of Relative Mitochondrial-Membrane Potential in Living Cells by Fluorescence Microscopy. *J. Cell Biol.* **1981**, *88*, 526−535.
(12) Minamikawa, T.; Sriratana, A.; Williams, D. A.; Bowser, D. N.; Hill, J. S.; Nagley, P. Chloromethyl-X-rosamine (MitoTracker Red) photosensitises mitochondria and induces apoptosis in intact human cells. *J. Cell Sci.* **1999**, *112*, 2419−2430.
(13) Shim, S. H.; Xia, C. L.; Zhong, G. S.; Babcock, H. P.; Vaughan, J. C.; Huang, B.; Wang, X.; Xu, C.; Bi, G. Q.; Zhuang, X. W. Super-resolution fluorescence imaging of organelles in live cells with photoswitchable membrane probes. *Proc. Natl. Acad. Sci. U.S.A.* **2012**, *109*, 13978−13983.
(14) Zhang, X. F.; Xiao, Y.; Qi, J.; Qu, J. L.; Kim, B.; Yue, X. L.; Belfield, K. D. Long-Wavelength, Photostable, Two-Photon Excitable BODIPY Fluorophores Readily Modifiable for Molecular Probes. *J. Org. Chem.* **2013**, *78*, 9153−9160.
(15) Jiang, N.; Fan, J. L.; Liu, T.; Cao, J. F.; Qiao, B.; Wang, J. Y.; Gao, P.; Peng, X. J. A near-infrared dye based on BODIPY for tracking morphology changes in mitochondria. *Chem. Commun.* **2013**, *49*, 10620−10622.
(16) Dodani, S. C.; Leary, S. C.; Cobine, P. A.; Winge, D. R.; Chang, C. J. A Targetable Fluorescent Sensor Reveals That Copper-Deficient SCO1 and SCO2 Patient Cells Prioritize Mitochondrial Copper Homeostasis. *J. Am. Chem. Soc.* **2011**, *133*, 8606−8616.
(17) Cheng, G. H.; Fan, J. L.; Sun, W.; Sui, K.; Jin, X.; Wang, J. Y.; Peng, X. J. A highly specific BODIPY-based probe localized in mitochondria for HClO imaging. *Analyst* **2013**, *138*, 6091−6096.
(18) Miao, F.; Zhang, W. J.; Sun, Y. M.; Zhang, R. Y.; Liu, Y.; Guo, F. Q.; Song, G. F.; Tian, M. G.; Yu, X. Q. Novel fluorescent probes for highly selective two-photon imaging of mitochondria in living cells. *Biosens. Bioelectron.* **2014**, *55*, 423−429.
(19) Han, J. H.; Park, S. K.; Lim, C. S.; Park, M. K.; Kim, H. J.; Kim, H. M.; Cho, B. R. Simultaneous Imaging of Mitochondria and Lysosomes by Using Two-Photon Fluorescent Probes. *Chem.—Eur. J.* **2012**, *18*, 15246−15249.
(20) Singha, S.; Kim, D.; Rao, A. S.; Wang, T.; Kim, K. H.; Lee, K. H.; Kim, K. T.; Ahn, K. H. Two-photon probes based on arylsulfonyl azides: Fluorescence detection and imaging of biothiols. *Dyes Pigm.* **2013**, *99*, 308−315.
(21) Yang, W. G.; Chan, P. S.; Chan, M. S.; Li, K. F.; Lo, P. K.; Mak, N. K.; Cheah, K. W.; Wong, M. S. Two-photon fluorescence probes for imaging of mitochondria and lysosomes. *Chem. Commun.* **2013**, *49*, 3428−3430.

(22) Dai, Y.; Lv, B. K.; Zhang, X. F.; Xiao, Y. A two-photon mitotracker based on a naphthalimide fluorophore: Synthesis, photophysical properties and cell imaging. *Chin. Chem. Lett.* **2014**, *25*, 1001−1005.
(23) Hori, Y.; Kikuchi, K. Protein labeling with fluorogenic probes for no-wash live-cell imaging of proteins. *Curr. Opin. Chem. Biol.* **2013**, *17*, 644−650.
(24) Lidell, M. E.; Betz, M. J.; Leinhard, O. D.; Heglind, M.; Elander, L.; Slawik, M.; Mussack, T.; Nilsson, D.; Romu, T.; Nuutila, P.; Virtanen, K. A.; Beuschlein, F.; Persson, A.; Borga, M.; Enerback, S. Evidence for two types of brown adipose tissue in humans. *Nat. Med.* **2013**, *19*, 631−634.
(25) Griffin, B. A.; Adams, S. R.; Tsien, R. Y. Specific covalent labeling of recombinant protein molecules inside live cells. *Science* **1998**, *281*, 269−272.
(26) Taylor, R. C.; Cullen, S. P.; Martin, S. J. Apoptosis: Controlled demolition at the cellular level. *Nat. Rev. Mol. Cell Biol.* **2008**, *9*, 231−241.
(27) Leung, C. W. T.; Hong, Y. N.; Chen, S. J.; Zhao, E. G.; Lam, J. W. Y.; Tang, B. Z. A Photostable AIE Luminogen for Specific Mitochondrial Imaging and Tracking. *J. Am. Chem. Soc.* **2013**, *135*, 62−65.
(28) Gao, M.; Sim, C. K.; Leung, C. W. T.; Hu, Q. L.; Feng, G. X.; Xu, F.; Tang, B. Z.; Liu, B. A fluorescent light-up probe with AIE characteristics for specific mitochondrial imaging to identify differentiating brown adipose cells. *Chem. Commun.* **2014**, *50*, 8312−8315.
(29) Hori, Y.; Norinobu, T.; Sato, M.; Arita, K.; Shirakawa, M.; Kikuchi, K. Development of Fluorogenic Probes for Quick No-Wash Live-Cell Imaging of Intracellular Proteins. *J. Am. Chem. Soc.* **2013**, *135*, 12360−12365.
(30) Zhuang, Y. D.; Chiang, P. Y.; Wang, C. W.; Tan, K. T. Environment-Sensitive Fluorescent Turn-On Probes Targeting Hydrophobic Ligand-Binding Domains for Selective Protein Detection. *Angew. Chem., Int. Ed.* **2013**, *52*, 8124−8128.
(31) Hovelmann, F.; Gaspar, I.; Ephrussi, A.; Seitz, O. Brightness Enhanced DNA FIT-Probes for Wash-Free RNA Imaging in Tissue. *J. Am. Chem. Soc.* **2013**, *135*, 19025−19032.
(32) Rosales, T.; Xu, J. H.; Wu, X. W.; Hodoseek, M.; Callis, P.; Brooks, B. R.; Knutson, J. R. Molecular dynamics simulations of perylene and tetracene librations: Comparison with femtosecond upconversion data. *J. Phys. Chem. A* **2008**, *112*, 5593−5597.
(33) Klymchenko, A. S.; Demchenko, A. P. 3-Hydroxychromone dyes exhibiting excited-state intramolecular proton transfer in water with efficient two-band fluorescence. *New J. Chem.* **2004**, *28*, 687−692.
(34) Ercelen, S.; Klymchenko, A. S.; Mely, Y.; Demchenko, A. P. The binding of novel two-color fluorescence probe FA to serum albumins of different species. *Int. J. Biol. Macromol.* **2005**, *35*, 231−242.
(35) Demchenko, A. P.; Mely, Y.; Duportail, G.; Klymchenko, A. S. Monitoring biophysical properties of lipid membranes by environment-sensitive fluorescent probes. *Biophys. J.* **2009**, *96*, 3461−3470.
(36) Verma, A. K.; Pratap, R. Chemistry of biologically important flavones. *Tetrahedron* **2012**, *68*, 8523−8538.
(37) Nijveldt, R. J.; van Nood, E.; van Hoorn, D. E. C.; Boelens, P. G.; van Norren, K.; van Leeuwen, P. A. M. Flavonoids: A review of probable mechanisms of action and potential applications. *Am. J. Clin. Nutr.* **2001**, *74*, 418−425.
(38) Magde, D.; Wong, R.; Seybold, P. G. Fluorescence quantum yields and their relation to lifetimes of rhodamine 6G and fluorescein in nine solvents: Improved absolute standards for quantum yields. *Photochem. Photobiol.* **2002**, *75*, 327−334.
(39) Klein, J.; Fasshauer, M.; Ito, M.; Lowell, B. B.; Benito, M.; Kahn, C. R. β_3-Adrenergic stimulation differentially inhibits insulin signaling and decreases insulin-induced glucose uptake in brown adipocytes. *J. Biol. Chem.* **1999**, *274*, 34795−34802.
(40) Qin, C. X.; Chen, X. Q.; Hughes, R. A.; Williams, S. J.; Woodman, O. L. Understanding the cardioprotective effects of flavonols: Discovery of relaxant flavonols without antioxidant activity. *J. Med. Chem.* **2008**, *51*, 1874−1884.
(41) Liu, B.; Wang, H.; Wang, T. S.; Bao, Y. Y.; Du, F. F.; Tian, J.; Li, Q. B. A.; Bai, R. K. A new ratiometric ESIPT sensor for detection of palladium species in aqueous solution. *Chem. Commun.* **2012**, *48*, 2867−2869.
(42) Liu, B.; Wang, J. F.; Zhang, G.; Bai, R. K.; Pang, Y. Flavone-Based ESIPT Ratiometric Chemodosimeter for Detection of Cysteine in Living Cells. *ACS Appl. Mater. Interfaces* **2014**, *6*, 4402−4407.
(43) Yamaguchi, T.; Asanuma, M.; Nakanishi, S.; Saito, Y.; Okazaki, M.; Dodo, K.; Sodeoka, M. Turn-ON fluorescent affinity labeling using a small bifunctional O-nitrobenzoxadiazole unit. *Chem. Sci.* **2014**, *5*, 1021−1029.
(44) Kucherak, O. A.; Richert, L.; Mely, Y.; Klymchenko, A. S. Dipolar 3-methoxychromones as bright and highly solvatochromic fluorescent dyes. *Phys. Chem. Chem. Phys.* **2012**, *14*, 2292−2300.
(45) Casey, J. R.; Grinstein, S.; Orlowski, J. Sensors and regulators of intracellular pH. *Nat. Rev. Mol. Cell Biol.* **2010**, *11*, 50−61.
(46) Hoye, A. T.; Davoren, J. E.; Wipf, P.; Fink, M. P.; Kagan, V. E. Targeting mitochondria. *Acc. Chem. Res.* **2008**, *41*, 87−97.
(47) de Graaf, A. O.; van den Heuvel, L. P.; Dijkman, H. B. P. M.; De Abreu, R. A.; Birkenkamp, K. U.; de Witte, T.; van der Reijden, B. A.; Smeitink, J. A. M.; Jansen, J. H. Bcl-2 prevents loss of mitochondria in CCCP-induced apoptosis. *Exp. Cell Res.* **2004**, *299*, 533−540.
(48) Martinou, J. C.; Youle, R. J. Mitochondria in Apoptosis: Bcl-2 Family Members and Mitochondrial Dynamics. *Dev. Cell* **2011**, *21*, 92−101.
(49) Simonsen, C. C.; Mcgrogan, M. The Molecular-Biology of Production Cell-Lines. *Biologicals* **1994**, *22*, 85−94.